RECENZIRANI ČLANKI | PEER-REVIEWED ARTICLES

Uporaba učenja s prenosom znanja za medregionalno kartiranje poljščin

Transfer Learning for Cross-Regional Crop Mapping

Miloš Pandžić, Dejan Pavlović, Oskar Marko, Milan Kilibarda

UDK: 528.9+633:004.85
Klasifikacija prispevka po COBISS.SI: 1.01
Prispelo: 20. 1. 2026
Sprejeto: 12. 3. 2026

DOI: https://doi.org/10.15292/geodetski-vestnik.2026.02.268-288
SCIENTIFIC ARTICLE
Received: 20. 1. 2026
Accepted: 12. 3. 2026

SI | EN

IZVLEČEK

Natančne informacije o prostorski porazdelitvi poljščin so bistvenega pomena za sodobno kmetijstvo, ki se zaradi podnebnih sprememb in svetovnega povpraševanja po hrani spopada z vse večjimi pritiski. Napredek pri opazovanju Zemlje, razpoložljivosti satelitskih podatkov in strojnem učenju (ang. machine learning – ML) je omogočil učinkovito spremljanje poljščin v velikem obsegu. Tradicionalni pristopi h kartiranju poljščin temeljijo na velikih naborih podatkov, kar je drago in zapleteno, zato se spodbuja uporaba alternativnih metod. Učenje s prenosom znanja (ang. transfer learning –TL) odpravlja to omejitev s prilagoditvijo modelov, naučenih na območjih, kjer je označenih podatkov veliko, na območja, kjer označenih podatkov ni ali pa jih je malo. V tej študiji preučujemo učenje TL za kartiranje vrst poljščin z uporabo naključnega gozda (ang.Random Forest – RF) in transformerja samo s kodirnikom z glavo klasifikacije v treh podatkovnih nizih: Sentinel-1, Sentinel-2 in njuni kombinaciji. Satelitske časovne vrste smo interpolirali v 15-dnevne intervale, da se zagotovi dosleden vhodni podatek. Modele smo učili na velikem označenem naboru podatkov iz Slovenije in jih prenesli v Srbijo. Ocenili smo standardne strategije prenosa modelov in natančnega prilagajanja. Najboljšo učinkovitost je dosegel pristop TL, ki je dosegel rezultat F1 91 % in za 7 % presegel nadzorovano merilo znotraj regije.

ABSTRACT

Accurate information on crop spatial distribution is essential for modern agriculture, which faces increasing pressure from global food demand and climate change. Advances in Earth observation, satellite data availability, and machine learning (ML) have enabled effective large-scale crop monitoring. Traditional crop mapping relies on large labeled datasets, which are often costly and difficult to obtain, necessitating the use of alternative strategies. Transfer learning (TL) addresses this limitation by enabling models trained in data-rich regions to be adapted to data-scarce regions. In this study, we investigate TL for crop type classification using Random Forest (RF) and encoder-only Transformer with a classification head across three data modalities: Sentinel-1, Sentinel-2, and their combination. Satellite time series were interpolated to regular 15-day intervals to ensure consistent model input. Models were trained on a large labeled dataset from Slovenia and transferred to Serbia, where labeled data is limited. We evaluated off-the-shelf model transfer and fine-tuning strategies. The best performance was achieved by a Transformer-based TL approach with a frozen feature extractor and fine-tuned classifier head, reaching an F1 score of 91% and outperforming the in-region supervised benchmark by 7%. These results demonstrate the potential of TL for cross-regional crop mapping in studied regions while substantially reducing reliance on large labeled datasets.

KLJUČNE BESEDE

prenos znanja, kartiranje poljščin, Sentinel-1, Sentinel-2, transformerji, naključni gozd

KEY WORDS

transfer learning, crop mapping, Sentinel-1, Sentinel-2, transformer, random forest

1 Introduction

Technological breakthroughs over the past decades have fundamentally transformed the way environmental information is acquired and processed. In Earth observation (EO), this transformation is evident in the rapid growth of satellite missions and data volumes (Xia et al., 2018; Wilkinson et al., 2024), further accelerated by open data policies adopted by agencies such as the National Aeronautics and Space Administration (NASA) and the European Space Agency (ESA), which made both new and legacy mission data freely available (Wulder et al., 2012; Aschbacher and Milagro-Pérez, 2012). In parallel, advances in machine learning (ML) have provided powerful tools for analyzing vast amounts of data (Nguyen et al., 2019), profoundly influencing numerous application domains.

In agriculture, the integration of EO data with advanced artificial intelligence techniques has enabled substantial modernization (Kamir et al., 2020; Jung et al., 2021; Ennouri et al., 2021; Benos et al., 2021; Victor et al., 2024). Among the most important EO-derived products are crop maps, which describe the spatial distribution of crops and support a wide range of stakeholders. In operational settings, these maps are used for supply chain planning, market analysis, policymaking, and monitoring the impacts of climate change on agricultural production, thereby contributing to a more sustainable and resilient agricultural sector and improved food security (UNOOSA and FAO, 2025). Crop maps are also essential for scientific research on agricultural trends (Potapov et al., 2022), climate impacts (Leng and Huang, 2017), and ecosystem dynamics (Baldassini et al., 2024).

Despite these advances, accurate and timely crop mapping remains challenging. Data-related and environmental constraints include limited image availability, cloud cover, scarcity of labeled data, agro-ecosystem complexity, spectral similarity between crops, spatial resolution limitations, soil interference, and other (Wu et al., 2023; Amani et al., 2020; Fei et al., 2024; Feyisa et al., 2020; Hegarty-Craver et al., 2020; Preidl et al., 2020; Yang et al., 2019; Teixeira et al., 2023; Wang et al., 2024b). On the other hand, more and more research nowadays is thoroughly investigating model-related challenges, particularly transferability (Pandžić et al., 2024; Račić et al., 2024; Wang et al., 2024b; Antonijević et al., 2023), explainability (Kopanja et al., 2024; Chan et al., 2023), and multimodal data integration (Garnot et al., 2022; Gadiraju et al., 2020; Karmakar et al., 2024; Shafi et al., 2020; Yan et al., 2021). Several of these aspects are addressed in this study.

Accurate crop mapping is strongly dependent on the availability and quality of ground truth (GT) data. While some European countries mandate crop-type declarations through subsidy programs (Arias et al., 2020) and provide open access to such data, other regions, lacking this protocol, remain understudied despite their agricultural potential (Pandžić et al., 2024). In these areas, GT is often collected through conventional field surveys, which are costly and labor-intensive, resulting in small proprietary datasets (Feyisa et al., 2020; Hegarty-Craver et al., 2020; Yang et al., 2019). Alternative unsupervised approaches, such as clustering combined with aggregated statistics, are limited by the availability and timeliness of official agricultural statistics, which still can be an issue in developing countries (Wang et al., 2019). The combined effect of limited labeled data and high variability in remote sensing observations has been shown to significantly affect ML model performance (Gadiraju and Vatsavai, 2023).

One way to mitigate these limitations is to reuse knowledge acquired in different regions or time periods for similar tasks. This concept, known as Transfer Learning (TL), enables models trained in one region to support crop mapping in target areas with limited training data (Hao et al., 2020). However, TL introduces additional challenges related to phenological differences, environmental and climatic variability (Orynbaikyzy et al., 2022; Hoppe et al., 2024; Wang et al., 2021), spectral inconsistencies, and data availability across regions. Wu et al. (2023) emphasize that TL methods should reduce the reliance on in situ data and minimize the need for extensive GT collection.

A strict definition of TL is found in Yang et al. (2020): "Given a source domain $\mathcal{D}_S$ and learning task $\mathcal{T}_S$, a target domain $\mathcal{D}_T$ and learning task $\mathcal{T}_T$, *transfer learning* aims to help improve the learning of the target predictive function $f_t(\cdot)$ in $\mathcal{D}_T$ using the knowledge in $\mathcal{D}_S$ and $\mathcal{T}_S$, where $\mathcal{D}_S \neq \mathcal{D}_T$ or $\mathcal{T}_S \neq \mathcal{T}_T$."

Building on this definition, numerous studies have investigated spatial and temporal TL for crop mapping. For instance, Antonijević et al. (2023) employed a Sentinel-2-based transductive transfer learning from France to Serbia, achieving successful results despite differences in class composition. Transductive TL refers to the setting in which knowledge is transferred across different but related domains while tasks remain the same (Pan and Yang, 2009). However, this term is sometimes used inconsistently in the literature and is occasionally conflated with unsupervised domain adaptation, which has led some authors to avoid the term (Yang et al., 2020). Similarly, Luo et al. (2022) trained a random forest model on data from England and France and also utilized transductive transfer learning to facilitate crop mapping in other European countries, while Keraani et al. (2022) evaluated transformer-based models transferred from France to Tunisia. Wang et al. (2019) transferred RF models across the US Midwest and confirmed that the more similar two nearby regions are, in terms of crop composition and growing conditions (measured with Growing Degree Days in their study), the higher is the accuracy achieved regarding model transfer. To address domain shift more explicitly, several studies proposed specialized adaptation strategies. Wang et al. (2023b) introduced a deep adaptation crop classification network (DACCN) to handle missing labels, Xu et al. (2020) applied an LSTM-based approach for dynamic crop mapping, and Che et al. (2024) proposed the DSH framework, combining DeepLabV3+, self-attention, and histogram matching to enhance generalization across multiple regions. Phenology-aware methods have also been explored. Ge et al. (2021) aimed to align few phenological stages prior to TL, and Wang et al. (2021) proposed a Phenology Alignment Network based on unsupervised domain adaptation (DA). Nyborg et al. (2022) introduced TimeMatch, an unsupervised DA approach that outperformed other DA methods but remained inferior to supervised learning. Hoppe et al. (2024) systematically evaluated the effects of spatial, temporal, and phenological differences on transferability. In addition to unsupervised DA, some studies propose a semi-supervised DA approach (Lucas et al., 2023), where some labeled samples are available in the target domain. Recent studies have further improved transferability through targeted correction mechanisms. Wang et al. (2024a) proposed SITS-based (satellite image time series) and temperature-based correction units to mitigate SITS shifts between domains, significantly boosting the performance of both RF and Transformer encoder models. Orynbaikyzy et al. (2022) enhanced RF transferability through spatial feature selection that was aimed at removing site-specific features. Alternative strategies include domain generalization via multi-season training (Rusnák et al., 2023) and the integration of crop rotation and local distribution data (Barriere et al., 2024). While these approaches often improve overall performance, they may do so at the expense of specific crop classes. Wang et al. (2023a) proposed Cropformer for multi-scenario mapping, though it showed limited success in spatial transfer settings. TL has also been applied using pretrained computer vision models. Gadiraju and Vatsavai (2023), Nowakowski et al. (2021), and Peng et al. (2024) successfully fine-tuned ImageNet-pretrained networks, such as VGG16, for remote sensing imagery.

A brief overview of TL crop mapping literature showed that the most frequently seen study areas are located in the United States and China, occasionally in EU member states, and seldom in other regions. The predominance of large, uniform fields in well-studied regions, contributes to disparity in literature, as these landscapes generally present a less complex classification task compared to the fragmented agricultural land commonly found in other regions. Most of the studies are published within the last five years adding on to its relevance. As seen, they vary considerably in terms of approaches, algorithms and performances, and sometimes in terminology (Nowakowski et al., 2024), occasionally leading to inconsistencies in interpretation, hence reflecting the evolving nature of the field. While this short overview focused solely on spatial TL, which in fact has already been recognized as prevalent in literature (Ma et al., 2024), readers interested in temporal TL, which is beyond the scope of the current investigation, are referred to studies such as You and Dong (2020), Hu et al. (2022), Rusnák et al. (2023), Yang et al. (2023), Račić et al. (2024), Pandžić et al. (2024), and Pham et al. (2024).

Motivated by previous work, we combine and extend several existing ideas to explore their joint potential for a specific use case. Our study briefly builds on concepts from Hao et al. (2020), who applied transfer learning using 15-day NDVI time series covering the full growing season, and Gadiraju and Vatsavai (2023), who compared crop-mapping strategies ranging from training models from scratch to using pre-trained convolutional neural networks as feature extractors or fine-tuning selected layers. We focus on classifying the same crop types in two regions (Slovenia and Vojvodina, Serbia) using satellite image time series and transfer-based approaches, including direct model transfer without target-domain samples and transfer learning with a limited number of target-domain samples for fine-tuning. These settings differ from standard crop-mapping practice, which typically relies on large labeled datasets from the target domain. The objectives of the study are following:

1. Investigate the applicability of transfer learning for cross-regional crop type mapping through a case study between Slovenia and Vojvodina (Serbia).
2. Evaluate the effectiveness of transfer learning strategies under limited in situ data availability and compare them with traditional crop mapping approaches (defined here as models trained and applied within the same region).
3. Analyze factors influencing the transferability of crop classification models across regions.

2 Data and Study Regions

2.1 Study regions

The Republic of Slovenia was selected as the source domain. Despite its small size (≈20,000 km²; Figure 1), Slovenia exhibits pronounced landscape heterogeneity due to diverse relief, climate, and agricultural practices (Račić et al., 2024). It spans four physiographic regions: Alpine, Dinarides, Mediterranean, and the Pannonian Basin, which dominates lowland agriculture in the northeast. The climate ranges from temperate humid to continental and Alpine (Komac et al., 2020), with mean annual precipitation of ~1,750 mm (ranging from ~3,000 mm in the northwest to ~700 mm in the northeast) and average temperatures between 8 and 11 °C. Dominant soils include Chromic Cambisol and Rendzina alternation, Dystric Cambisol and Eutric Cambisol, generally rich in humus but affected by degradation (Zorn et al., 2020). Agriculture covers about 34% of the country, with

37% arable crops (MKGP, 2024), characterized by small, fragmented, and irregular parcels (Račić et al., 2024).

The Autonomous Province of Vojvodina was selected as the target domain. Covering ~21,500 km² in northern Serbia (Figure 1), it is predominantly agricultural, with arable land occupying about 73% of the area (Galić et al., 2009). Located in the southeastern Pannonian Basin, the region is flat (70–130 m elevation) and highly fertile (Hrnjak et al., 2014), with soils such as Chernozems, Arenosols, Fluvisols, Vertisols, and Solonetz (Ćirić et al., 2020). The temperate climate features hot humid summers, cold winters, uneven rainfall, and strong temperature extremes, with a mean annual temperature of ~11 °C and precipitation around 600 mm (Hrnjak et al.; 2014, Gavrilov et al., 2015; Tošić et al., 2014). Climate change impacts are increasingly evident, including higher drought and flood risk (Jachia and Milovanović, 2022) and a shift toward warmer Köppen climate zones (Mimić et al., 2024). Agricultural parcels are also highly fragmented (Pandžić et al., 2024).

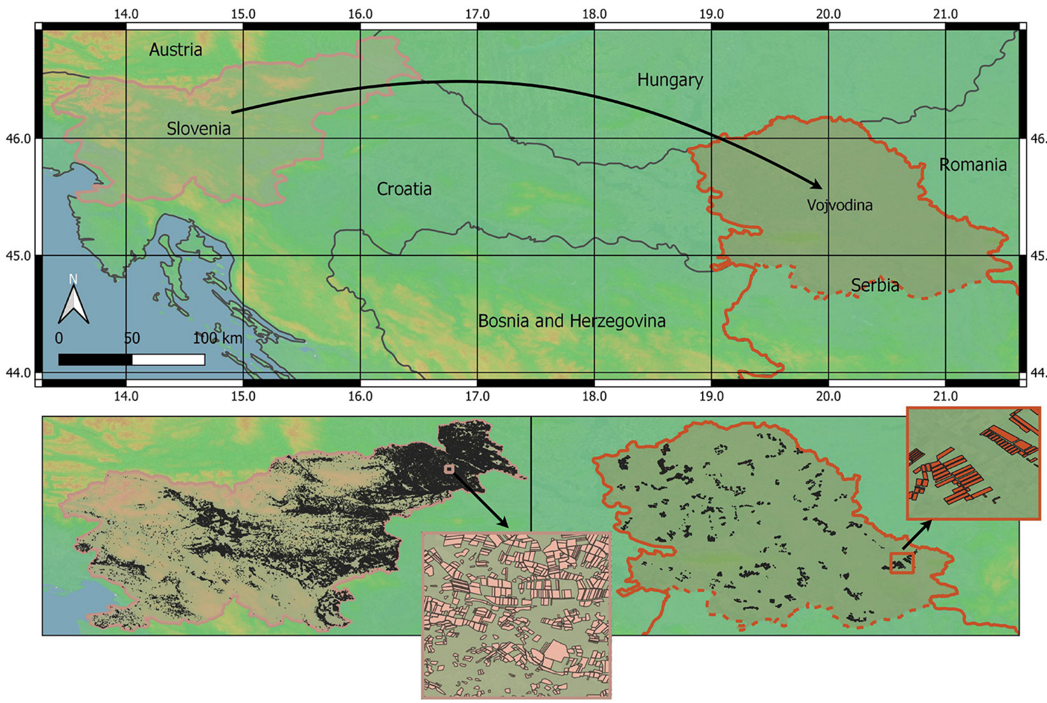

Figure 1: Location of study regions and the direction of model transfer (upper image). Distribution of ground truth samples per region (lower images). There are 159,533 parcels for Slovenia and 2,399 for Serbia. Distance between centroids of the two regions is approximately 420 km.

2.2 Ground truth

Ground truth (GT) data for Slovenia were obtained from the Ministry of Agriculture, Forestry and Food of Slovenia (MKGP-Portal, 2021), based on mandatory farmer declarations. Nine crop types were selected to match those in Vojvodina: corn, wheat, soybean, sunflower, sugar beet, oilseed rape, barley, clover, and orchard (Pandžić et al., 2024). The final Slovenian dataset contained 159,533 parcels, covering nearly 50% of arable land.

In Serbia, where mandatory crop declarations are not in place, GT data were collected through field campaigns conducted in late May and early July 2021 (Pandžić et al., 2024). Field surveys prioritized large, homogeneous parcels to minimize border effects and maximize labeled pixel counts. Parcel locations, geotagged crop images, and metadata were collected using an in-house mobile application, followed by manual digitization in QGIS (2022) using Sentinel-2 imagery. Ambiguous records were removed. The final Serbian dataset comprised 2,399 parcels, covering approximately 3.5% of arable land, highlighting the labor-intensive and costly nature of GT collection and motivating the use of transfer learning.

Summary statistics are provided in Table 1, crop type distributions in Figure 2, and parcel size distribution comparisons in Figure 3.

Table 1: Summary statistics for ground truth and satellite imagery databases given per study region. Provided are: number of parcels, average and median size of parcels, area covered by GT, percentage of total arable land covered by GT, number of Sentinel-2 and Sentinel-1 acquisitions.

Study region	# Parcels	Avg. size (ha)	Median size (ha)	GT area (km²)	% Area covered	S2 images	S1 images
Slovenia	159,533	0.78	0.46	1,245.28	49.5%	617	324
Serbia	2,399	23.25	14.53	557.75	3.5%	510	303

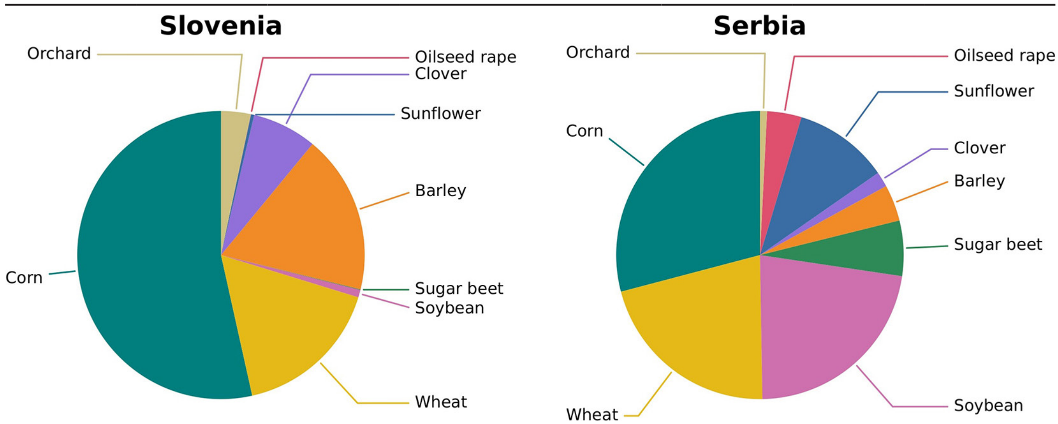

Figure 2: Crop type distribution in two regions: Slovenia with 159,533 samples and Serbia with 2,399 samples.

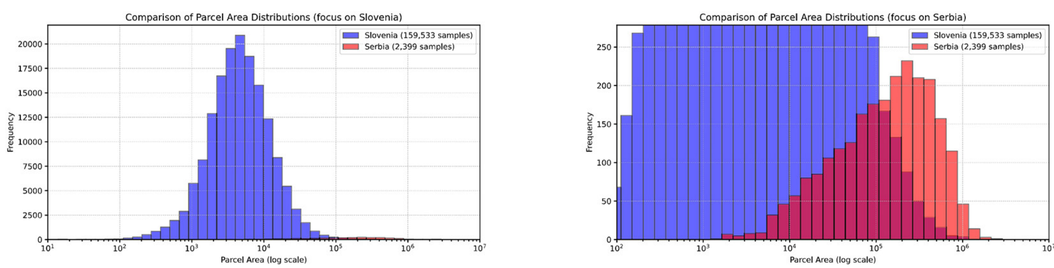

Figure 3: Comparison of parcel area distribution between Slovenia and Serbia. The image on the left shows a full scene, while the image on the right shows a zoomed-in view at a specific range to highlight details that are not clearly visible in the left image.

2.3 Satellite data

Sentinel-2 is the European Space Agency's (ESA) multispectral optical mission currently consisting of three satellites (Sentinel-2A, 2B, and 2C), launched in 2015, 2017, and 2024, operating in sun-synchronous orbit at 786 km altitude with a nominal 5-day revisit time (SentiWiki-s2, 2024). Each satellite carries a Multi-Spectral Instrument (MSI) with 13 bands covering the visible, red-edge, near-infrared, short-wave infrared, and atmospheric regions at spatial resolutions of 10–60 m (Pahlevan et al., 2017). Its wide swath (290 km) and open data policy boosted agricultural and environmental applications.

Sentinel-1 is the ESA's C-band SAR mission, originally comprising Sentinel-1A and 1B, launched in 2014 and 2015 (Sentinel-1B was decommissioned in 2022), operating at ~693 km altitude with a 6-day revisit time at the constellation level (Potin et al., 2016; Pandžić et al., 2020; SentiWiki-s1, 2024). Follow-on satellites Sentinel-1C and 1D ensure mission continuity. Operating at 5.405 GHz, Sentinel-1 provides all-weather, day-and-night observations with dual polarization and multiple acquisition modes. In this study, Level-1 GRD products acquired in Interferometric Wide Swath (IW) mode were used, with ~250 km swath width and incidence angles between 29.1° and 46.0°. Sentinel-1 data are also distributed under a free and open data policy.

2.4 Google Earth Engine and initial data preprocessing

Sentinel-1 and Sentinel-2 data were accessed via Google Earth Engine (GEE), a cloud-based geospatial analysis platform hosting over 90 PB of analysis-ready satellite data empowered by Google Cloud's computational capabilities and analytic tools (Gorelick et al., 2017; Cloud, 2024). For Sentinel-2, Level-2A surface reflectance products were selected, and cloud and cloud shadow masking was performed using the Cloud Score+ quality assessment product (Pasquarella et al., 2023). Median per-parcel values were computed for each of 12 Sentinel-2 spectral bands (excluding band 10 used only for atmospheric correction) and ten vegetation indices (Table 2). Sentinel-1 GRD data, preprocessed by Google for thermal noise, radiometric calibration and terrain correction, were additionally processed with border noise correction, radiometric terrain normalization, and mono-temporal Lee speckle filtering (kernel size 5), following Pandžić et al. (2024) and using code from Mullissa et al. (2021). This resulted in Gamma0 backscatter as output and median per-parcel values were extracted for VH and VV polarizations and their ratio. Hence, including both sensors, a total of 25 raster layers (i.e. features) were used for processing, all layers were resampled to 10 m resolution, and data from April 1 to September 30 corresponding to the 2021 growing season were used. Though GEE supports advanced ML workflows, it was used here solely for data access and dataset generation, following Gorelick (2024).

Table 2: Selection of ten commonly used vegetation indices included in the experiment based on their relevance in remote sensing applications, particularly vegetation monitoring. B# represent respective Sentinel-2 bands.

Vegetation Index	Formula	Short Description	Reference
Normalized Difference Vegetation Index	$NDVI = \frac{B8 - B4}{B8 + B4}$	Most widely used vegetation index that quantifies the greenness and health of vegetation by comparing the reflectance of near-infrared and red wavelengths.	(Kriegler, 1969)
Enhanced Vegetation Index	$EVI = 2.5 \times \frac{B8 - B4}{B8 + 6 \cdot B4 - 7.5 \cdot B2 + 1}$	Designed to minimize atmospheric influences and enhance sensitivity to canopy structural variations.	(Huete et al., 2002)
Two-Band Enhanced Vegetation Index	$EVI2 = 2.5 \times \frac{B8 - B4}{B8 + 2.4 \cdot B4 + 1}$	An alternative to EVI when sensor does not have blue band.	(Jiang et al., 2008)
Normalized Difference Moisture Index	$NDMI = \frac{B8a - B11}{B8a + B11}$	Suitable for monitoring plant water content. (Often mistaken for NDWI, which uses green and NIR bands.)	(Gao, 1996)
Soil-Adjusted Vegetation Index	$SAVI = \frac{B8 - B4}{B8 + B4 + L}(1 + L), L = 0.5$	Minimizes soil brightness influences by incorporating a soil adjustment factor (L) into the calculation.	(Huete, 1988)
Plant Senescence Reflectance Index	$PSRI = \frac{B4 - B2}{B6}$	Quantifies the degree of plant senescence based on reflectance properties of chlorophyll and carotenoid pigments.	(Merzlyak et al., 1999)
Sentinel-2 LAI_{green} Index	$SeLI = \frac{B8a - B5}{B8a + B5}$	Designed to estimate Leaf Area Index (LAI) from Sentinel-2 satellite imagery.	(Pasqualotto et al., 2019)
Atmospherically Resistant Vegetation Index	$ARVI = \frac{B8 - B4 - \gamma(B4 - B2)}{B8 + B4 + \gamma(B4 - B2)}$	Designed to minimize effects of atmospheric scattering.	(Kaufman and Tanre, 1992)
Excess Green Index	$ExG = 2 \cdot B3 - B4 - B2$	Used for detecting vegetation stress by highlighting green vegetation areas.	(Woebbecke et al., 1995)
Chlorophyll Red Edge Index	$Chl\_red\_edge = \frac{B7}{B5} - 1$	Used as an indicator of chlorophyll content.	(Gitelson et al., 2003)

3 Methodology

In this research, cross-regional transfer learning for crop mapping using optical and radar satellite image time series is in focus. Nine crop types are classified using two different algorithms, Random Forest and Transformer Encoder. Transfer learning approach is compared against simple transfer (i.e. when pretrained model is used off-the-shelf without further adaptations; hereafter referred to as naïve), as well as against traditional crop mapping approach, in order to assess and eventually justify its use with respect to final results. Selected approaches ensure reproducibility and allow systematic evaluation of transfer learning strategies in the presented case study. The following subsections address each aspect of the methodology in detail.

3.1 Data preprocessing

Using GEE-stored satellite imagery and parcel geometry from ground truth data, initial datasets were generated by extracting the median pixel value of the parcel when intersected with a satellite image, for each band. This process was repeated for all parcels, considering each pixel and every available satellite image in the time series (except for those excluded on the basis of Cloud Score+ due to high cloud cover). Equation (1) describes this process:

$$\tilde{X}_{c,t}^{(i),v} = median\left(\left\{x_{c,t,p}^{v} \,\middle|\, p \in P_i, P_i \subset \mathcal{D}_{r,v} \cap \mathcal{P}_r, c \in C_v, t \in T_i\right\}\right) \quad (1)$$

where:

$\tilde{X}_{c,t}^{(i),v}$ - median pixel value for parcel *i* (of region *r*), channel *c*, at date *t*, within modality *v*,

$median(\cdot)$ - function computing the median of pixel values,

$x_{c,t,p}^{v}$ - pixel value at position *p* (within parcel *i*), for channel *c*, at time *t*, in modality *v*,

P_i - a set of valid pixels belonging to parcel *i*, which is, in addition, a subset of intersection between two databases $\mathcal{D}_{r,v} \cap \mathcal{P}_r$:

$\mathcal{D}_{r,v}$ - the satellite imagery database defined by region $r \in \{SLO, SRB\}$ and modality $v \in \{S1, S2, S1 + S2\}$, i.e. Sentinel-1, Sentinel-2 or combination of the two,

$\mathcal{P}_r$ - the parcel database for region $r \in \{SLO, SRB\}$, i.e. either Slovenia or Serbia,

C_v - the set of available channels under specific modality *v* (either C_{S1}, C_{S1} or C_{S1+S2}),

T_i - initial set of observed time points for parcel *i* (before interpolation).

As previously indicated, Slovenian data served as the source domain while Serbian data served as the target domain. Since the number of acquisitions, as well as the very dates of acquisitions, could vary between the two test areas (or even between parcels of the same region), and especially having in mind varying cloud cover over the regions that affect the usability of images, it was decided to preprocess downloaded data in order to achieve the time series of the same length, without gaps. For this reason, we applied cubic spline interpolation integrated in the SciPy library (Virtanen et al., 2020), and selected dates at a 15-day interval. Instead of extrapolating, in the case of missing data at the beginning or end of the time period, forward and backward padding was used. This preprocessing was performed on all data resulting in an even number of features between the two domains with respect to satellite sensor type, i.e. Sentinel-1, Sentinel-2, or combination of both. Interpolation process can be described by equation (2):

$$\hat{X}_{c,t}^{(i),v} = \begin{cases} \tilde{X}_{c,t_1}^{(i),v}, & if\ t < t_1\,(FP) \\ \mathcal{I}\left(\left\{\left(t_k, \tilde{X}_{c,t_k}^{(i),v}\right)\right\}_{k=1}^{K}\right), & t_1 \le t \le t_K\,(CSI) \\ \tilde{X}_{c,t_K}^{(i),v}, & if\ t > t_K\,(BP) \end{cases} \tag{2}$$

where:

$\hat{X}_{c,t}^{(i),v}$ - interpolated values,

$\left\{\left(t_k, \tilde{X}_{c,t_k}^{(i),v}\right)\right\}_{k=1}^{K}$ - the original set of observed time points t_k and their corresponding median values before interpolation,

K - the number of available time points for parcel i before interpolation,

$\mathcal{I}(\cdot)$ - the cubic spline interpolation function,

t_1 - the first time point in the original satellite image time series for i-th parcel

t_K - the last time point in the original satellite image time series for i-th parcel

$t \in T_{15}$ - the new resampled set of time points (i.e., dates selected at a 15-day interval),

$FP(t < t_1)$ - forward padding where the earliest observed value is assigned,

$BP(t > t_K)$ - backward padding where the latest observed value is assigned, and

CSI - cubic spline interpolation.

3.2 Kolmogorov–Smirnov test

Since in this case source and target tasks are the same (i.e. classification of nine identical crop types), in order to be able to discuss transfer learning after all, it was necessary first to check if source and target domains are truly different. They can be considered different if their feature spaces differ $\mathcal{X}_S \neq \mathcal{X}_T$, or their marginal probability distributions $P(X_S) \neq P(X_T)$, where $X_{S_i} \in \mathcal{X}_S$ and $X_{T_i} \in \mathcal{X}_T$ (Yang et al., 2020). In this case, the feature spaces are identical due to preprocessing described in the previous section, so it was necessary to assess the identity of the marginal probability distributions by comparing corresponding samples (i.e., pairs of features) from the two domains. One way to determine if the two probability distributions are significantly different is to use the Kolmogorov–Smirnov (KS) test. Kolmogorov–Smirnov test is a nonparametric method used to determine whether the two samples are drawn from the same underlying distribution (Kottegoda and Rosso, 2008). Test statistic is calculated as:

$$D = \sqrt{\frac{mn}{m+n}} \cdot D_{m,n} \tag{3}$$

where

$$D_{m,n} = \sup_x \left| F_m(x) - G_n(x) \right| \tag{4}$$

with F_m and G_n denoting the empirical distribution functions of two samples (source domain and target domain) of sizes m and n, respectively. The term *sup* refers to the supremum function. The null hypothesis posits that both samples share the same underlying distribution. It is rejected in case of the test's p-value being less than the level of significance, which is set to $\alpha = 0.05$ for all tests.

3.3 Algorithms

Two algorithms were selected: **Random Forest (RF)** and **Transformer Encoder (TR)**. RF represents a well-established machine learning baseline widely used in crop classification, while Transformers represent state-of-the-art deep learning architectures.

Random Forest is an ensemble learning method that constructs multiple decision trees using random subsets of samples and features, thus enhancing diversity while reducing overfitting. Predictions are obtained by aggregating outputs of individual trees, typically via majority voting for classification tasks (Breiman, 2001).

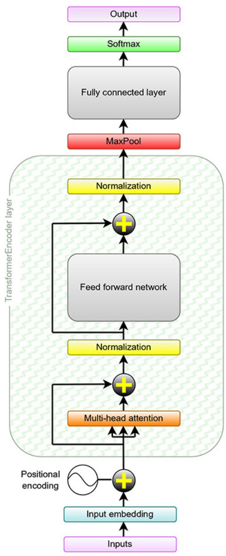

Figure 4: Modified Transformer architecture utilized in the experiment.

Table 3: Hyperparameter selection process using grid search, except for learning rate chosen at random under uniform distribution. Parameters: n_estimators - number of trees; max_depth - maximum tree depth; min_samples_leaf - minimum leaf size; d_model - dimensionality of the hidden states; n_head - number of heads in the multi-head attention mechanism; n_layers - number of encoder layers; dropout - dropout probability.

Algorithm	Hyperparameter	Values
RF	n_estimators	[100, 500, 1000]
	max_depth	[1, 5, 10, 50]
	min_samples_leaf	[1, 5 ,10, 50, 100]
TR	d_model	[2^6, 2^7, 2^8, 2^9]
	n_head	[2^0, 2^1, 2^2, 2^3]
	n_layers	[2^0, 2^1, 2^2, 2^3]
	dropout	[0, 0.1, 0.25]
	learning_rate	[1e-2, 1e-3, 1e-4, 1e-5]

Transformers are neural network architectures based on the self-attention mechanism designed for sequential data (Vaswani et al., 2017). The attention mechanism enables the model to determine how much importance (i.e. weight) each element in the input sequence has on processing other elements of the sequence, making Transformers suitable for SITS classification where relationships across different times or features matter. Although originally formulated as encoder–decoder architectures, only the encoder was used in this study. Input embeddings were retained to project data into higher-dimensional spaces, while positional encoding was applied to preserve temporal order. A final classification head mapped encoder outputs to crop labels (Figure 4).

3.4 Experiment design

Experiments were conducted using three data modalities: **Sentinel-1 only (S1)**, **Sentinel-2 only (S2)**, and their **combination (S1+S2)**. Identical strategies were applied across modalities.

The Slovenian dataset was split into 70% training, 15% validation, and 15% testing using stratified sampling, ensuring parcels (with all their belonging pixels) were assigned exclusively to one subset to prevent data leakage. The Serbian dataset was split into 15% training, 15% validation, and 70% testing to simulate a realistic scenario of limited target-domain ground truth availability. The experimental workflow is illustrated in Figure 5.

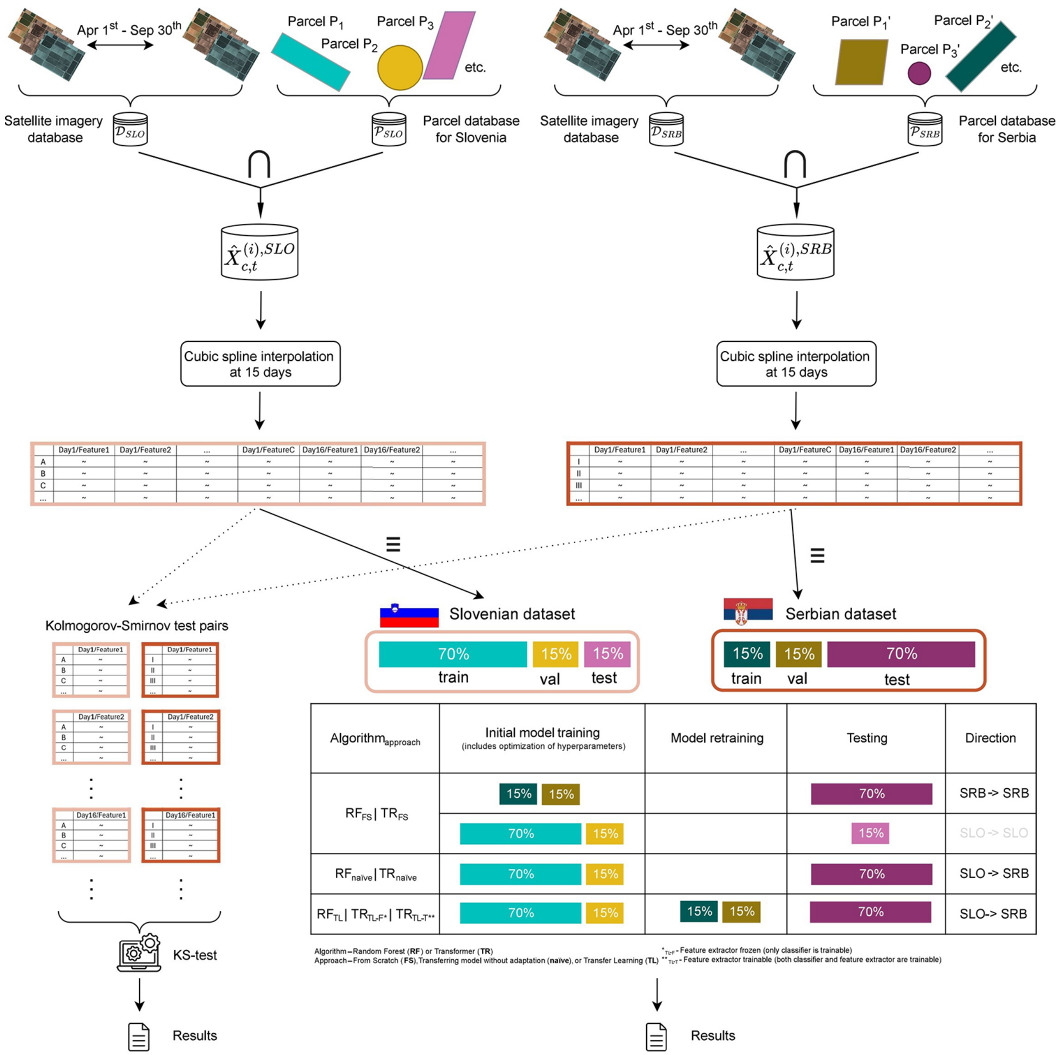

Figure 5: Experiment workflow. It starts off by obtaining a time series of satellite imagery for all pixels and parcels in two domains, Slovenia and Serbia. Images are acquired from Google Earth Engine for period April 1st to September 30th, and cloudy pixels were excluded based on Cloud Score+ value. Then, the median value of each parcel in each time step was calculated, followed by cubic spline interpolation with a 15-day interval in order to obtain a regular and complete time series dataset. Pairs of features from two domain datasets were used in Kolmogorov-Smirnov tests (dashed arrows). For the rest of experimentation, Slovenian dataset was split into 70%, 15%, 15%, and Serbian dataset into 15%, 15%, 70%, respectively for training, validation and testing. Investigated scenarios and corresponding data to use are given in bottom-right part of image. Algorithms: RF - random forest, TR - transformer; In subscript: FS - from scratch, naïve - off-the-shelf algorithm, TL - transfer learning, F - frozen feature extractor, T - fully trainable model.

Hyperparameter optimization was performed independently for each algorithm (RF or TR), modality (S1, S2, S1 + S2) and domain (Serbia or Slovenia) combination, resulting in 12 optimization runs (one run for each combination, e.g. hyperparameter optimization of RF for Sentinel-1 data for Serbia). Looking up to previous work (Vaswani et al., 2017; Yuan and Lin, 2020; Rußwurm and Körner, 2020; Xu et al., 2020; Pandžić et al., 2024), RF hyperparameters included number of trees, maximum tree depth, and minimum leaf size, while TR hyperparameters included number of attention heads, hidden states dimensionality, number of encoder layers, and dropout rate, with the inner feedforward dimension fixed at four times the hidden size. Grid search, which systematically tests every possible hyperparameter combination, was used, resulting in 60 RF and 192 TR configurations (Table 3), each evaluated via five-fold cross-validation. Learning rate (LR), which can play a crucial role in model performance, did not yield adequate results on initial runs that used variable LR. Hence, we decided to go with a predefined set, spanning several orders of magnitude. Rather than exhaustively combining all LR values with every other hyperparameter, configurations were sampled using uniform distribution to maintain a computationally tractable search space, given the high training cost of individual optimization runs (often several days long). In this way we still ensured to analyze both small and large learning rates in combination with both simple and complex models, encompassing thus overall optimization performance variations. The **F1 score** was used as the primary selection metric due to class imbalance, providing a balanced measure of Precision and Recall (Eq. 5). Best-performing models from each optimization run were selected for further experiments.

$$F1\ score = 2 \cdot \frac{Precision \cdot Recall}{Precision + Recall} = \frac{2 \cdot TP}{2 \cdot TP + FP + FN} \tag{5}$$

TP - True Positives; FP - False Positives; FN - False Negatives

Models trained and tested within the same domain were labeled **from scratch** (RF_{FS}, TR_{FS}), with Serbian FS results serving as benchmarks. **Naïve transfer** ($RF_{naïve}$, $TR_{naïve}$) involved applying Slovenian pretrained models directly to Serbia without adaptation (off-the-shelf). **Transfer learning (TL)** combined Slovenian pretrained models with limited Serbian data. For RF, TL involved adding new trees trained on Serbian samples (RF_{TL}). For Transformers, two TL variants were tested: retraining only the classifier head while feature extractor was frozen (TR_{TL-F}) and fine-tuning all layers (TR_{TL-T}).

4 Results

4.1 Kolmogorov–Smirnov test

To assess domain similarity, 325 Kolmogorov-Smirnov tests were performed on feature-wise marginal probability distributions. The null hypothesis of identical distributions was rejected in 324 cases ($p < \frac{\alpha}{N_{test}}$), confirming statistically significant differences between the source (Slovenia) and target (Serbia) domains. This result validates the prerequisite for employing transfer learning techniques in this study.

4.2 Crop mapping

Optimal hyperparameters are summarized in Table 4. RF configurations showed stable parameter choices, while TR configurations exhibited higher variability.

Results for crop mapping are given in Table 5. Benchmark results (FS on Serbian data) achieved F1 scores between **76–84%** for RF and **76–83%** for TR, with best performance obtained using combined S1+S2 data. These results represent realistic performance under limited in situ data availability.

Naïve transfer led to substantial performance degradation, with maximum F1 scores of **46% (RF)** and **67% (TR)**. Compared to source-domain performance, this reflects notable drops, particularly for RF, highlighting limited generalization without adaptation.

Transfer learning significantly improved performance. RF-TL achieved F1 scores up to **87%**, exceeding the benchmark by 3%. Transformer-based TL performed best, reaching **91% F1** using S1+S2 data, surpassing the benchmark by 7%. Differences between frozen and fully trainable Transformer variants were minimal. Only S1-based Transformer TL underperformed relative to the benchmark.

Confusion matrices (Figure 6) show that TL improved classification for most crops compared to naïve transfer, especially soybean, sugar beet, oilseed rape, and orchard. Remaining confusion primarily involved barley and wheat.

Table 4: Results of hyperparameter optimization given per algorithm, domain and modality. Algorithms: RF - random forest, TR - transformer; Domains: SLO - Slovenia, SRB - Serbia; Modalities: S1 - Sentinel-1, S2 - Sentinel-2, S1+S2 - Sentinel-1 and Sentinel-2.

Algorithm	Domain	Modality	Parameters
RF	SLO	S1	n_estimators: 1000, max_depth: 50, min_samples_leaf: 1
		S2	n_estimators: 1000, max_depth: 50, min_samples_leaf: 1
		S1+S2	n_estimators: 1000, max_depth: 50, min_samples_leaf: 1
	SRB	S1	n_estimators: 1000, max_depth: 50, min_samples_leaf: 1
		S2	n_estimators: 1000, max_depth: 50, min_samples_leaf: 1
		S1+S2	n_estimators: 100, max_depth: 50, min_samples_leaf: 1
TR	SLO	S1	n_head: 2, output_dim: 128, num_encoder_layers: 4, dropout: 0, learning_rate: 0.001
		S2	n_head: 2, output_dim: 256, num_encoder_layers: 8, dropout: 0.1, learning_rate: 0.0001
		S1+S2	n_head: 8, output_dim: 64, num_encoder_layers: 8, dropout: 0.25, learning_rate: 0.001
	SRB	S1	n_head: 4, output_dim: 128, num_encoder_layers: 4, dropout: 0, learning_rate: 0.001
		S2	n_head: 2, output_dim: 64, num_encoder_layers: 4, dropout: 0, learning_rate: 0.001
		S1+S2	n_head: 2, output_dim: 64, num_encoder_layers: 4, dropout: 0, learning_rate: 0.001

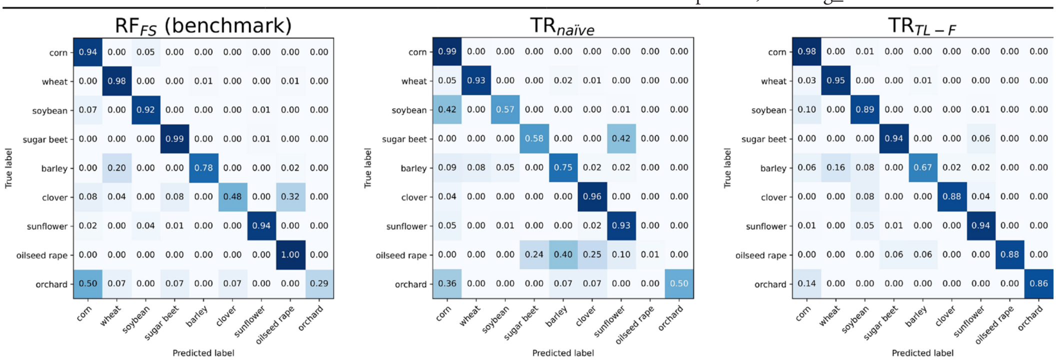

Figure 6: Confusion matrices for the benchmark model (left), the best performing model of naïve approach (middle), and the best performing transfer learning model (right). All three are given for S1+S2 modality.

Table 5: The F1 score, Precision, Recall, and Overall Accuracy (OA) for different algorithm approaches. Scenarios in gray text are added to offer a more complete perspective on the results, even though they have a different test set (SLO -> SLO direction cases). Algorithms: RF - random forest, TR - transformer. In subscript: FS - from scratch, naive - off-the-shelf algorithm, TL - transfer learning, F - frozen feature extractor, T - fully trainable model.

$Algorithm_{approach}$	Direction	Modality											
		S1				S2				S1+S2			
		F1 score	Precision	Recall	OA	F1 score	Precision	Recall	OA	F1 score	Precision	Recall	OA
RF_{FS}	SRB → SRB	76.34%	93.29%	73.93%	90.48%	79.17%	90.53%	76.82%	91.19%	84.35%	93.58%	81.37%	93.27%
	SLO → SLO	39.22%	56.00%	35.91%	77.24%	60.90%	77.90%	55.41%	89.72%	62.88%	77.89%	57.28%	90.04%
TR_{FS}	SRB → SRB	76.10%	79.58%	74.71%	85.18%	83.04%	88.12%	80.41%	90.12%	76.51%	80.62%	74.58%	88.27%
	SLO → SLO	48.47%	60.17%	44.33%	77.85%	68.92%	73.08%	66.13%	90.79%	72.23%	74.29%	70.63%	91.14%
$RF_{naïve}$	SLO → SRB	35.12%	52.49%	40.91%	52.56%	40.67%	66.34%	50.02%	55.42%	46.49%	67.84%	53.72%	60.06%
$TR_{naïve}$	SLO → SRB	42.68%	48.81%	49.59%	58.99%	57.98%	79.51%	63.59%	76.61%	66.80%	81.08%	69.17%	79.64%
RF_{TL}	SLO → SRB	85.62%	93.74%	82.89%	89.64%	83.76%	91.73%	81.41%	86.67%	87.34%	93.53%	85.81%	89.76%
TR_{TL-F}	SLO → SRB	72.95%	84.30%	69.36%	81.96%	89.39%	92.45%	86.93%	92.02%	91.11%	93.89%	88.77%	92.80%
TR_{TL-T}	SLO → SRB	75.31%	84.40%	72.41%	82.32%	90.08%	93.67%	87.61%	93.33%	90.62%	93.99%	88.61%	94.29%

5 Discussion

KS tests confirmed significant differences between the two geographical regions, driven by differences in climate, topography, management practices, and image availability. Against this backdrop, TL proved effective in transferring crop mapping knowledge from Slovenia to Serbia.

Transformer-based TL using combined optical and radar data yielded the best performance (91% F1), confirming the benefit of multimodal inputs. Comparable performance between fully retrainable Transformers and those with some frozen layers suggests that pretrained representations already captured transferable features. Weaker results for S1-only Transformers indicate limitations of radar-only data in this context, while RF benefited more consistently from S1 inputs due to fuller utilization of limited Serbian samples. To clarify, Transformers used 15% of the Serbian data for training and another 15% for validation, whereas RF used the full 30% (i.e. the same 15% + 15%) solely for training, potentially capturing more useful information. In addition, radar backscatter signals are inherently noisier and less directly linked to crop biophysical properties than optical measurements, which may favor simpler models when the available training data are limited. The combined influence of speckle-noise-prone-data and the limited number of samples available for retraining may affect complex models such as Transformers more severely than simpler ones like RF, potentially hindering effective model optimization. Furthermore, the RF transfer learning strategy combines trees trained on both the source and target domains within a single ensemble, whereas Transformer-based transfer learning relies on the adaptation of pretrained weights. With a limited number of samples and noisy inputs, such fine-tuning may provide insufficient capacity for effective adaptation, potentially resulting in lower performance despite the initial quality of the pretrained model. Lower FS performance in Slovenia compared to Serbia is attributed to parcel fragmentation and mixed pixels (Figure 3), as well as terrain-induced radar distortions. Naïve transfer performed poorly, thus reinforcing findings about unlikely off-the-shelf universal crop mapping models (Hoppe et al., 2024; Barriere et al., 2024).

Class-wise results show that transfer learning benefits mainly those crops underrepresented in source domain (oilseed rape, sugar beet, orchard and soybean). The good discrimination in the naïve approach for corn, wheat, clover, and sunflower, indicates more transferable spectral-temporal patterns of these crops. Performance trade-offs under TL were limited and mainly affected barley and, to a lesser extent, clover, likely due to phenological similarity with wheat and differing regional management practices, such as occasional double cropping in Serbia.

Although direct comparison with previous studies is complicated by differences in experimental design (Rusnák et al., 2023), our findings are broadly consistent with existing literature. For instance, Orynbaikyzy et al. (2022) showed that combining optical and radar data improves performance across regions, a conclusion generally derivable from our results. Our benchmark results are in line with theirs, and while their spatial transfer outperformed our respective naïve approach, it was surpassed by our Transformer-based TL model, highlighting the benefit of adaptation beyond simple transfer. Our results also align well with Gadiraju and Vatsavai (2023), who demonstrated that pretrained initialization, including selective layer freezing strategies, can outperform training from scratch in limited-data scenarios. Despite architectural differences, both studies report comparable performance levels and similar relative gains from TL. Consistent findings were reported by Antonijević et al. (2023), who achieved comparable accuracy when transferring Sentinel-2-based models from France to Vojvodina, and by Barriere et al. (2024), whose results converge toward ours as target-domain labeled data availability increases. Finally, agreement is observed with Nyborg et al. (2022), who reported a clear gap between unsupervised and fully supervised transferring approaches, with performance ranges and method rankings similar to those obtained in this study. Naïve transferring was the only unsupervised approach in our study, and while higher accuracies have been reported using more advanced unsupervised DA techniques (Ge et al., 2021; Xu et al., 2020; Wang et al., 2021; Rusnák et al., 2023; Wang et al., 2024a), classification problems were often much simpler, and these approaches still typically require additional data preprocessing or model modifications. Overall, our results fall well within the range reported in prior work, reinforcing TL as a robust and practical strategy for cross-regional crop mapping.

6 Conclusion

This study demonstrated that transfer learning could substantially improve cross-regional crop mapping when target-domain ground truth is scarce. Under limited Serbian training data (15%), the benchmark from-scratch models achieved F1 scores between 76–84%, while naïve transfer dropped performance to 46% (RF) and 67% (TR), confirming strong domain shift. In contrast, transfer learning increased performance up to 87% for RF and 91% for Transformer Encoder models (using combined Sentinel-1 and Sentinel-2 data), surpassing the benchmark by as much as 7 percentage points. Transformer-based TL therefore outperformed traditional RF-based crop mapping, providing strong justification for continued exploration of these methods in future. The experimental setup relies solely on freely available Sentinel-1 and Sentinel-2 data and standardized time series generation, thus mitigating the problem of irregular data acquisitions due to e.g. cloudiness, and allowing for replication of the study in other regions. To further validate the effectiveness of the investigated transfer learning strategies, additional experiments across multiple regions and seasons are required. The obtained results provide empirical support for the expectation that TL performance may further improve between more similar regions and suggest that certain crop types may exhibit higher cross-regional transferability. While the growing body of TL studies confirms the potential, the current lack of standardization in crop mapping TL research presents a burden towards reaching more impactful breakthroughs in this area. Future work will explore additional modalities (e.g., weather and phenology), in-season crop mapping, and simplified yet robust TL models.

Data availability

A full crop type parcel information dataset for Slovenia is available at https://rkg.gov.si/vstop/. Crop type parcel information dataset for Serbia is proprietary dataset of the BioSense Institute, and parts or full dataset may be shared upon the assessment of individual requests. Satellite images for both Sentinel-1 and Sentinel-2 are available on Google Earth Engine (https://earthengine.google.com/).

Software availability

Codes are made publicly available at the following repository to ensure full transparency and reproducibility of the methodology https://github.com/milospandzic/TL_4_crossregional_crop_mapping.

Acknowledgments

This work was supported by the Ministry of Education, Science and Technological Development of the Republic of Serbia (Grant No. 451-03-136/2025-03/ 200358). The authors would also like to express their gratitude to Dr. Noel Gorelick, one of the founders of Google Earth Engine, for his help and valuable comments regarding the platform.

References

Amani, M., Kakooei, M., Moghimi, A., Ghorbanian, A., Ranjgar, B., Mahdavi, S., Davidson, A., Fisette, T., Rollin, P., Brisco, B., et al., 2020. Application of google earth engine cloud computing platform, sentinel imagery, and neural networks for crop mapping in Canada. Remote Sensing 12, 3561.

Antonijević, O., Jelić, S., Bajat, B., Kilibarda, M., 2023. Transfer learning approach based on satellite image time series for the crop classification problem. Journal of Big Data 10, 54.

Arias, M., Campo-Bescós, M.Á., Álvarez-Mozos, J., 2020. Crop classification based on temporal signatures of sentinel-1 observations over Navarre Province, Spain. Remote Sensing 12, 278.

Aschbacher, J., Milagro-Pérez, M.P., 2012. The european earth monitoring (gmes) programme: Status and perspectives. Remote Sensing of Environment 120, 3–8.

Baldassini, P., Sans, G.C., Segura, D.A., Conde, C., Paruelo, J.M., 2024. Mapping cropping systems and their effects on ecosystem functioning and services in the argentine pampas. Agriculture, Ecosystems & Environment 369, 109027.

Barriere, V., Claverie, M., Schneider, M., Lemoine, G., d'Andrimont, R., 2024. Boosting crop classification by hierarchically fusing satellite, rotational, and contextual data. Remote Sensing of Environment 305, 114110.

Benos, L., Tagarakis, A.C., Dolias, G., Berruto, R., Kateris, D., Bochtis, D., 2021. Machine learning in agriculture: A comprehensive updated review. Sensors 21, 3758.

Breiman, L., 2001. Random forests. Machine learning 45, 5–32.

Chan, A., Schneider, M., Körner, M., 2023. Xai for early crop classification, in: IGARSS 2023-2023 IEEE International Geoscience and Remote Sensing Symposium, IEEE. pp. 2657–2660.

Che, H., Pan, Y., Xia, X., Zhu, X., Li, L., Huang, Y., Zheng, X., Wang, L., 2024. A new transferable deep learning approach for crop mapping. GIScience & Remote Sensing 61, 2395700.

Ćirić, V.I., Manojlović, M.S., Nešić, L.M., Belić, M.Đ., 2020. Depth distribution of organic matter concentration and stocks in soils of vojvodina. Zbornik Matice srpske za prirodne nauke , 19–29.

Cloud, G., 2024. Analyze satellite imagery and geospatial data at planetary scale, howpublished = https://cloud. google.com/earth-engine?hl=en. (accessed on 27 August 2024).

Ennouri, K., Smaoui, S., Gharbi, Y., Cheffi, M., Ben Braiek, O., Ennouri, M., Triki, M.A., 2021. Usage of artificial intelligence and remote sensing as efficient devices to increase agricultural system yields. Journal of Food Quality 2021, 6242288.

Fei, C., Li, Y., McNairn, H., Lampropoulos, G., 2024. Early-season crop classification utilizing time series based deep learning with multi-sensor remote sensing data, in: IGARSS 2024-2024 IEEE International Geoscience and Remote Sensing Symposium, IEEE. pp. 4132–4135.

Feyisa, G.L., Palao, L.K., Nelson, A., Gumma, M.K., Paliwal, A., Win, K.T., Nge, K.H., Johnson, D.E., 2020. Characterizing and mapping cropping patterns in a complex agro-ecosystem: An iterative participatory mapping procedure using machine learning algorithms and modis vegetation indices. Computers and electronics in agriculture 175, 105595.

Gadiraju, K.K., Ramachandra, B., Chen, Z., Vatsavai, R.R., 2020. Multimodal deep learning based crop classification using multispectral and multitemporal satellite imagery, in: Proceedings of the 26th ACM SIGKDD International Conference on knowledge discovery & data mining, pp. 3234–3242.

Gadiraju, K.K., Vatsavai, R.R., 2023. Remote sensing based crop type classification via deep transfer learning. IEEE Journal of Selected Topics in Applied Earth Observations and Remote Sensing 16, 4699–4712.

Galić, Z., Orlović, S., Galović, V., Poljaković-Pajnik, L., Pap, P., Vasić, V., 2009. Challenges of land use change and land protection in vojvodina. Afr J Agric Res 4, 1566–1573.

Gao, B.C., 1996. Ndwi-a normalized difference water index for remote sensing of vegetation liquid water from space. Remote sensing of environment 58, 257–266.

Garnot, V.S.F., Landrieu, L., Chehata, N., 2022. Multi-modal temporal attention models for crop mapping from satellite time series. ISPRS Journal of Photogrammetry and Remote Sensing 187, 294–305.

Gavrilov, M.B., Marković, S.B., Jarad, A., Korać, V.M., 2015. The analysis of temperature trends in Vojvodina (Serbia) from 1949 to 2006. Thermal Science 19, 339–350.

Ge, S., Zhang, J., Pan, Y., Yang, Z., Zhu, S., 2021. Transferable deep learning model based on the phenological matching principle for mapping crop extent. International Journal of Applied Earth Observation and Geoinformation 102, 102451.

Gitelson, A.A., Gritz, Y., Merzlyak, M.N., 2003. Relationships between leaf chlorophyll content and spectral reflectance and algorithms for non-destructive chlorophyll assessment in higher plant leaves. Journal of plant physiology 160, 271–282.

Gorelick, N., 2024. Fast(er) Downloads, howpublished = https://gorelick.medium. com/ fast-er-downloads-a2abd512aa26. (accessed on 15 April 2024).

Gorelick, N., Hancher, M., Dixon, M., Ilyushchenko, S., Thau, D., Moore, R., 2017. Google earth engine: Planetaryscale geospatial analysis for everyone. Remote sensing of Environment 202, 18–27.

Hao, P., Di, L., Zhang, C., Guo, L., 2020. Transfer learning for crop classification with cropland data layer data (cdl) as training samples. Science of The Total Environment 733, 138869.

Hegarty-Craver, M., Polly, J., O'Neil, M., Ujeneza, N., Rineer, J., Beach, R.H., Lapidus, D., Temple, D.S., 2020. Remote crop mapping at scale: Using satellite imagery and uav-acquired data as ground truth. Remote Sensing 12, 1984.

Hoppe, H., Dietrich, P., Marzahn, P., Weiß, T., Nitzsche, C., Freiherr von Lukas, U., Wengerek, T., Borg, E., 2024. Transferability of machine learning models for crop classification in remote sensing imagery using a new test methodology: A study on phenological, temporal, and spatial influences. Remote Sensing 16, 1493.

Hrnjak, I., Lukić, T., Gavrilov, M.B., Marković, S.B., Unkašević, M., Tošić, I., 2014. Aridity in Vojvodina, Serbia. Theoretical and applied climatology 115, 323–332.

Hu, Y., Zeng, H., Tian, F., Zhang, M., Wu, B., Gilliams, S., Li, S., Li, Y., Lu, Y., Yang, H., 2022. An interannual transfer learning approach for crop classification in the hetao irrigation district, china. Remote Sensing 14, 1208.

Huete, A., Didan, K., Miura, T., Rodriguez, E.P., Gao, X., Ferreira, L.G., 2002. Overview of the radiometric and biophysical performance of the modis vegetation indices. Remote sensing of environment 83, 195–213.

Huete, A.R., 1988. A soil-adjusted vegetation index (savi). Remote sensing of environment 25, 295–309.

Jachia, L., Milovanović, J., 2022. Thematic update sustainable food systems. URL: \url{https://serbia. un.org/sites/default/files/2022-03/Copy%20of%20serbia. un_.org%20%2817%29.pdf}. (accessed on 1 September 2022).

Jiang, Z., Huete, A.R., Didan, K., Miura, T., 2008. Development of a two-band enhanced vegetation index without a blue band. Remote sensing of Environment 112, 3833–3845.

Jung, J., Maeda, M., Chang, A., Bhandari, M., Ashapure, A., Landivar-Bowles, J., 2021. The potential of remote sensing and artificial intelligence as tools to improve the resilience of agriculture production systems. Current Opinion in Biotechnology 70, 15–22.

Kamir, E., Waldner, F., Hochman, Z., 2020. Estimating wheat yields in australia using climate records, satellite image time series and machine learning methods. ISPRS Journal of Photogrammetry and Remote Sensing 160, 124–135.

Karmakar, P., Teng, S.W., Murshed, M., Pang, S., Li, Y., Lin, H., 2024. Crop monitoring by multimodal remote sensing: A review. Remote Sensing Applications: Society and Environment 33, 101093.

Kaufman, Y.J., Tanre, D., 1992. Atmospherically resistant vegetation index (arvi) for eos-modis. IEEE transactions on Geoscience and Remote Sensing 30, 261–270.

Keraani, M.K., Mansour, K., Khlaifia, B., Chehata, N., 2022. Few shot crop mapping using transformers and transfer learning with sentinel-2 time series: case of kairouan tunisia. The International Archives of the Photogrammetry, Remote

Sensing and Spatial Information Sciences 43, 899–906.

Komac, B., Pavšek, M., Topole, M., 2020. Climate and weather of slovenia. The Geography of Slovenia: Small But Diverse , 71–89.

Kopanja, M., Pejak, B., Radulović, M., Brdar, S., 2024. Shap-guided explanations for the machine learning classification of irrigated fields using satellite imagery. doi:10.5281/zenodo.10952482.

Kottegoda, N.T., Rosso, R., 2008. Goodness-of-Fit Tests. Wiley-Blackwell. pp. 270–283. ISBN: 978-1-405-17917-1.

Kriegler, F.J., 1969. Preprocessing transformations and their effects on multispectral recognition, in: Proceedings of the Sixth International Symposium on Remote Sesning of Environment, pp. 97–131.

Leng, G., Huang, M., 2017. Crop yield response to climate change varies with crop spatial distribution pattern. Scientific Reports 7, 1463.

Lucas, B., Pelletier, C., Schmidt, D., Webb, G.I., Petitjean, F., 2023. A bayesian-inspired, deep learning-based, semisupervised domain adaptation technique for land cover mapping. Machine Learning 112, 1941–1973.

Luo, Y., Zhang, Z., Zhang, L., Han, J., Cao, J., Zhang, J., 2022. Developing high-resolution crop maps for major crops in the european union based on transductive transfer learning and limited ground data. Remote Sensing 14, 1809.

Ma, Y., Chen, S., Ermon, S., Lobell, D.B., 2024. Transfer learning in environmental remote sensing. Remote Sensing of Environment 301, 113924.

Merzlyak, M.N., Gitelson, A.A., Chivkunova, O.B., Rakitin, V.Y., 1999. Non-destructive optical detection of pigment changes during leaf senescence and fruit ripening. Physiologia plantarum 106, 135–141.

Mimić, G., Podraščanin, Z., Basarin, B., 2024. Change detection of the köppen climate zones in southeastern europe.ˇ Atmospheric Science Letters 25, e1270.

MKGP, 2024. Slovenian agriculture, food, fishery and forestry in numbers. "Brochure". URL: \url{https://www.gov.si/assets/ministrstva/MKGP/PODROCJA/KMETIJSTVO/ EN-brochure-agriculture-in-numbers-2024.pdf}. (accessed on 16 May 2025).

MKGP-Portal, 2021. Graficni podatki KMRS - zbirna vloga 2021 za celo Slovenijo (shape.rar 180 MB) KoordSistem:ˇ D96/TM. https://rkg.gov.si/vstop/. (accessed on 1 June 2024).

Mullissa, A., Vollrath, A., Odongo-Braun, C., Slagter, B., Balling, J., Gou, Y., Gorelick, N., Reiche, J., 2021. Sentinel-1 sar backscatter analysis ready data preparation in google earth engine. Remote Sensing 13, 1954.

Nguyen, G., Dlugolinsky, S., Bobák, M., Tran, V., López García, Á., Heredia, I., Malík, P., Hluchy, L., 2019. Machine` learning and deep learning frameworks and libraries for large-scale data mining: a survey. Artificial Intelligence Review 52, 77–124.

Nowakowski, A., Del Rosso, M.P., Zachar, P., Spiller, D., Gabara, G., Barretta, D., Kalinowska, K.B., Choromanski, K., Wilkowski, A., Sebastianelli, A., et al., 2024. Transfer learning in earth observation data analysis: A review. IEEE Geoscience and Remote Sensing Magazine.

Nowakowski, A., Mrziglod, J., Spiller, D., Bonifacio, R., Ferrari, I., Mathieu, P.P., Garcia-Herranz, M., Kim, D.H., 2021. Crop type mapping by using transfer learning. International Journal of Applied Earth Observation and Geoinformation 98, 102313.

Nyborg, J., Pelletier, C., Lefèvre, S., Assent, I., 2022. Timematch: Unsupervised cross-region adaptation by temporal shift estimation. ISPRS Journal of Photogrammetry and Remote Sensing 188, 301–313.

Orynbaikyzy, A., Gessner, U., Conrad, C., 2022. Spatial transferability of random forest models for crop type classification using Sentinel-1 and sentinel-2. Remote Sensing 14, 1493.

Pahlevan, N., Sarkar, S., Franz, B.A., Balasubramanian, S.V., He, J., 2017. Sentinel-2 multispectral instrument (msi) data processing for aquatic science applications: Demonstrations and validations. Remote sensing of environment 201, 47–56.

Pan, S.J. and Yang, Q., 2009. A survey on transfer learning. IEEE Transactions on knowledge and data engineering, 22(10), pp.1345-1359.

Pandžić, M., Ljubičić, N., Mimić, G., Pandžić, J., Pejak, B., Crnojević, V., 2020. A case study of monitoring maize dynamics in serbia by utilizing Sentinel-1 data and growing degree days. ISPRS Annals of the Photogrammetry, Remote Sensing and Spatial Information Sciences , 117–124.

Pandžić, M., Pavlović, D., Matavulj, P., Brdar, S., Marko, O., Crnojević, V., Kilibarda, M., 2024. Interseasonal transfer learning for crop mapping using Sentinel-1 data. International Journal of Applied Earth Observation and Geoinformation 128, 103718.

Pasqualotto, N., Delegido, J., Van Wittenberghe, S., Rinaldi, M., Moreno, J., 2019. Multi-crop green lai estimation with a new simple sentinel-2 lai index (seli). Sensors 19, 904.

Pasquarella, V.J., Brown, C.F., Czerwinski, W., Rucklidge, W.J., 2023. Comprehensive quality assessment of optical satellite imagery using weakly supervised video learning, in: Proceedings of the IEEE/CVF Conference on Computer Vision and Pattern Recognition, pp. 2125–2135.

Peng, M., Liu, Y., Khan, A., Ahmed, B., Sarker, S.K., Ghadi, Y.Y., Bhatti, U.A., Al-Razgan, M., Ali, Y.A., 2024. Crop monitoring using remote sensing land use and land change data: Comparative analysis of deep learning methods using pre-trained cnn models. Big Data Research 36, 100448.

Pham, V.D., Tetteh, G., Thiel, F., Erasmi, S., Schwieder, M., Frantz, D., van der Linden, S., 2024. Temporally transferable crop mapping with temporal encoding and deep learning augmentations. International Journal of Applied Earth Observation and Geoinformation 129, 103867.

Potapov, P., Turubanova, S., Hansen, M.C., Tyukavina, A., Zalles, V., Khan, A., Song, X.P., Pickens, A., Shen, Q., Cortez, J., 2022. Global maps of cropland extent and change show accelerated cropland expansion in the twenty-first century. Nature Food 3, 19–28.

Potin, P., Rosich, B., Grimont, P., Miranda, N., Shurmer, I., O'Connell, A., Torres, R., Krassenburg, M., 2016. Sentinel-1 mission status, in: Proceedings of EUSAR 2016: 11th European Conference on Synthetic Aperture Radar, VDE. pp. 1–6.

Preidl, S., Lange, M., Doktor, D., 2020. Introducing apic for regionalised land cover mapping on the national scale using sentinel-2a imagery. Remote Sensing of Environment 240, 111673.

QGIS, 2022. QGIS A Free and Open Source Geographic Information System. https://www.qgis.org/en/site/. (accessed on 1 September 2022).

Racić, M., Oštir, K., Zupanc, A.,Čehovin Zajc, L., 2024. Multi-year time series transfer learning: Application of early crop classification. Remote Sensing 16, 270.

Rusnák, T., Kasanicky, T., Malík, P., Mojžiš, J., Zelenka, J., Svicek, M., Abrahám, D., Halabuk, A., 2023. Crop mapping without labels: Investigating temporal and spatial transferability of crop classification models using a 5-year sentinel-2 series and machine learning. Remote Sensing 15, 3414.

Rußwurm, M., Körner, M., 2020. Self-attention for raw optical satellite time series classification. ISPRS journal of photogrammetry and remote sensing 169, 421–435.

SCIHUB, 2022. End of mission of the Copernicus Sentinel-1B satellite. https://scihub.copernicus.eu/news/ News01067. (accessed on 1 September 2022).

SentiWiki-s1, 2024. Overview of Sentinel-1 Mission, howpublished = https://sentiwiki.copernicus.eu/web/ s1-mission. (accessed on 27 August 2024).

SentiWiki-s2, 2024. Overview of sentinel-2 mission. https://sentiwiki.copernicus.eu/web/s2-mission# S2-Mission-Spectral-Resolution. (accessed on 27 August 2024).

Shafi, U., Mumtaz, R., Iqbal, N., Zaidi, S.M.H., Zaidi, S.A.R., Hussain, I., Mahmood, Z., 2020. A multi-modal approach for crop health mapping using low altitude remote sensing, internet of things (iot) and machine learning. IEEE Access 8, 112708–112724.

Teixeira, I., Morais, R., Sousa, J.J., Cunha, A., 2023. Deep learning models for the classification of crops in aerial imagery: A review. Agriculture 13, 965.

Tošić, I., Hrnjak, I., Gavrilov, M.B., Unkašević, M., Marković, S.B., Lukić, T., 2014. Annual and seasonal variability of precipitation in vojvodina, serbia. Theoretical and applied climatology 117, 331–341.

UNOOSA, FAO, 2025. Leveraging space technology for agricultural development and food security,

https://openknowledge.fao.org/items/e8613797-6ef1-4e56-b854-d14cbada8660. (accessed on 12 February 2025).

Vaswani, A., Shazeer, N., Parmar, N., Uszkoreit, J., Jones, L., Gomez, A.N., Kaiser, Ł., Polosukhin, I., 2017. Attention is all you need. Advances in neural information processing systems 30.

Victor, B., Nibali, A., He, Z., 2024. A systematic review of the use of deep learning in satellite imagery for agriculture. IEEE Journal of Selected Topics in Applied Earth Observations and Remote Sensing .

Virtanen, P., Gommers, R., Oliphant, T.E., Haberland, M., Reddy, T., Cournapeau, D., Burovski, E., Peterson, P., Weckesser, W., Bright, J., van der Walt, S.J., Brett, M., Wilson, J., Millman, K.J., Mayorov, N., Nelson, A.R.J., Jones, E., Kern, R., Larson, E., Carey, C.J., Polat, ˙I., Feng, Y., Moore, E.W., VanderPlas, J., Laxalde, D., Perktold, J., Cimrman, R., Henriksen, I., Quintero, E.A., Harris, C.R., Archibald, A.M., Ribeiro, A.H., Pedregosa, F., van Mulbregt, P., SciPy 1.0 Contributors, 2020. SciPy 1.0: Fundamental Algorithms for Scientific Computing in Python.

Nature Methods 17, 261–272. doi:10.1038/s41592-019-0686-2.

Wang, H., Chang, W., Yao, Y., Yao, Z., Zhao, Y., Li, S., Liu, Z., Zhang, X., 2023a. Cropformer: A new generalized deep learning classification approach for multi-scenario crop classification. Frontiers in plant science 14, 1130659.

Wang, H., Ye, Z., Yao, Y., Chang, W., Liu, J., Zhao, Y., Li, S., Liu, Z., Zhang, X., 2024a. Improving cross-regional model transfer performance in crop classification by crop time series correction. Geo-spatial Information Science , 1–16.

Wang, S., Azzari, G., Lobell, D.B., 2019. Crop type mapping without field-level labels: Random forest transfer and unsupervised clustering techniques. Remote sensing of environment 222, 303–317.

Wang, Y., Feng, L., Zhang, Z., Tian, F., 2023b. An unsupervised domain adaptation deep learning method for spatial and temporal transferable crop type mapping using sentinel-2 imagery. ISPRS Journal of Photogrammetry and Remote Sensing 199, 102–117.

Wang, Y., Huang, H., State, R., 2024b. Cross domain early crop mapping using cropstgan. IEEE Access

Wang, Z., Zhang, H., He, W., Zhang, L., 2021. Phenology alignment network: A novel framework for cross-regional time series crop classification, in: Proceedings of the IEEE/CVF Conference on Computer Vision and Pattern Recognition, pp. 2940–2949.

Wilkinson, R., Mleczko, M., Brewin, R., Gaston, K., Mueller, M., Shutler, J., Yan, X., Anderson, K., 2024. Environmental impacts of earth observation data in the constellation and cloud computing era. Science of the Total Environment 909, 168584.

Woebbecke, D.M., Meyer, G.E., Von Bargen, K., Mortensen, D.A., 1995. Color indices for weed identification under various soil, residue, and lighting conditions. Transactions of the ASAE 38, 259–269.

Wu, B., Zhang, M., Zeng, H., Tian, F., Potgieter, A.B., Qin, X., Yan, N., Chang, S., Zhao, Y., Dong, Q., et al., 2023. Challenges and opportunities in remote sensing-based crop monitoring: A review. National Science Review 10, nwac290.

Wulder, M.A., Masek, J.G., Cohen, W.B., Loveland, T.R., Woodcock, C.E., 2012. Opening the archive: How free data has enabled the science and monitoring promise of landsat. Remote Sensing of Environment 122, 2–10.

Xia, J., Yang, C., Li, Q., 2018. Building a spatiotemporal index for earth observation big data. International journal of applied earth observation and geoinformation 73, 245–252.

Xu, J., Zhu, Y., Zhong, R., Lin, Z., Xu, J., Jiang, H., Huang, J., Li, H., Lin, T., 2020. Deepcropmapping: A multitemporal deep learning approach with improved spatial generalizability for dynamic corn and soybean mapping. Remote Sensing of Environment 247, 111946.

Yan, S., Yao, X., Zhu, D., Liu, D., Zhang, L., Yu, G., Gao, B., Yang, J., Yun, W., 2021. Large-scale crop mapping from multi-source optical satellite imageries using machine learning with discrete grids. International Journal of Applied Earth Observation and Geoinformation 103, 102485.

Yang, G., Li, X., Liu, P., Yao, X., Zhu, Y., Cao, W., Cheng, T., 2023. Automated in-season mapping of winter wheat in china with training data generation and model transfer. ISPRS Journal of Photogrammetry and Remote Sensing 202, 422–438.

Yang, N., Liu, D., Feng, Q., Xiong, Q., Zhang, L., Ren, T., Zhao, Y., Zhu, D., Huang, J., 2019. Large-scale crop mapping based on machine learning and parallel computation with grids. Remote Sensing 11, 1500.

Yang, Q., Zhang, Y., Dai, W., Pan, S.J., 2020. Transfer Learning, Introduction. Cambridge University Press. p. 3–22. doi:10.1017/9781139061773.003.

You, N., Dong, J., 2020. Examining earliest identifiable timing of crops using all available sentinel 1/2 imagery and google earth engine. ISPRS Journal of Photogrammetry and Remote Sensing 161, 109–123.

Yuan, Y., Lin, L., 2020. Self-supervised pretraining of transformers for satellite image time series classification. IEEE Journal of Selected Topics in Applied Earth Observations and Remote Sensing 14, 474–487.

Zorn, M., Breg Valjavec, M., Komac, B., Volk Bahun, M., Hrvatin, M., 2020. Soils of slovenia. The Geography of Slovenia: Small But Diverse , 91–107.

Pandžić M., Pavlović D., Marko O., Milan Kilibarda M. (2026). Transfer Learning for Cross-Regional Crop Mapping.
Geodetski vestnik, 70 (2), 268-288.
DOI: https://doi.org/geodetski-vestnik.2026.02.268-288

Miloš Pandžić, Ph.D. Candidate
BioSense Institute, University of Novi Sad,
Dr Zorana Đinđića 1, 21000 Novi Sad, Serbia
e-mail: milos.pandzic@biosense.rs

Oskar Marko, Ph.D.
BioSense Institute, University of Novi Sad,
Dr Zorana Đinđića 1, 21000 Novi Sad, Serbia
e-mail: oskar.marko@biosense.rs

Dejan Pavlović, Ph.D. Candidate
BioSense Institute, University of Novi Sad,
Dr Zorana Đinđića 1, 21000 Novi Sad, Serbia
e-mail: dejan.pavlovic@biosense.rs

Prof. Milan Kilibarda, Ph.D
University of Belgrade, Faculty of Civil Engineering
Bulevar kralja Aleksandra 73, 11000 Belgrade, Serbia
e-mail: kili@grf.bg.ac.rs